Applied Catalysis B: Environmental 168-169 (2015) 175–182

Contents lists available at ScienceDirect

Applied Catalysis B: Environmental

journal homepage: www.elsevier.com/locate/apcatb

Photocatalytic degradation and decomposition mechanism of fluoroquinolones norfloxacin over bismuth tungstate: Experiment and mathematic model

Meijuan Chen, W. Chu*

Department of Civil and Environmental Engineering, Research Centre for Urban Environmental Technology and Management, The Hong Kong Polytechnic University, Hung Hom, Kowloon, Hong Kong

ARTICLE INFO

Article history:
Received 13 October 2014
Received in revised form
11 December 2014
Accepted 16 December 2014
Available online 18 December 2014

Keywords:
Bi_2WO_6
Active species
Reaction mechanism
Mathematical model

ABSTRACT

Identification the active species and reaction intermediates during the treatment of norfloxacin using Bi_2WO_6 photocatalysis were investigated in this study. To the best of our knowledge this is the first study on the active species and reaction intermediates for the degradation of any fluoroquinolones (FQs) using Bi_2WO_6 photocatalysis. The role of active species was determined by the influence of radicals' scavengers and selected ions. The overall efficiency of Bi_2WO_6 photocatalysis was ascribed to photolysis, photocatalysis-via hydroxyl radical (•OH), and photocatalysis-via direct hole (h^+) oxidation, and their contribution was determined to be 15.0, 79.3, and 5.7%, respectively. Fourteen intermediates were identified in the treated samples. Among them, the five amide intermediates in Bi_2WO_6 photocatalysis were resulted from the OH oxidation on the piperazine in FQs. A reaction formula was developed to describe this reaction where amine translated into amide by the attack of OH radicals. Moreover, a mathematical model was successfully built up to predict the intermediates accumulation as the concentration of initial probe and reaction time is given, which is useful in practical application.

1. Introduction

The recent public interest regarding the presence of antibiotic pollutants in water has raised important concerns due to the unknown environmental impact and possible damages to the botany and fauna present in aquatic systems. One of the most consumed antibiotics corresponding to the classification of the fluoroquinolones (FQs) shows an annual consumption of more than 44 million in the world [1]. The FQs have been widely used to treat bacterial infections in humans and animals [2,3], which subsequently enter into aquatic environments through body excretion after administration [4]. Norfloxacin(1-ethyl-6-fluoro-4-oxo-7-piperazin-1-yl-1H-quinoline -3-carboxylic acid), a second generation of synthetic FQs, has been widely detected in the aqueous environment in Hong Kong due to its large prescription [5]. The ubiquity of norflxacin leads to serious concerns about the adverse effects on aquatic ecology and human health. The presence of norfloxacin in aquatic environment has reported to interfere with bacterial DNA replication, be toxic to aquatic plants and organism, and contribute to bacterial geno-toxicity [6,7]. Furthmore, the widespread norfloxacin in water might result in the development and spread of antibiotic resistant bacteria and resistance genes, which is regarded as one of the three greatest threats to human health by the World Health Organization [8].

Compared to other conventional chemical oxidation methods, photocatalysis is more effective in water treatment because of its important features, including (1) ambient operating temperature and pressure, (2) complete mineralization of parents and their intermediates without secondary pollution, and (3) low operating cost [9–14]. In the past decades, the use of TiO_2 as a catalyst for the clean up of environmental organic pollutants through the activation of the UV light has been widely studied. However, TiO_2 can only be excited by UV light with an irradiation wavelength less than 380 nm, leading to a compulsory artificial UV light source for initializing the process [15]. Concerning about energy conservation, solar light has been considered as a free and abundant source of great potential for new technology. Recently, researchers have reported many photocatalysts showing good performance by the solar light excited [16,17]. In particular, Bi_2WO_6 is known as the excellent one with higher removal efficiency on environmental pollutants [18], such as dyes [19] and bisphenol A [20].

* Corresponding author. Tel.: +852 2766 6075; fax: +852 2334 6389.
E-mail address: cewchu@polyu.edu.hk (W. Chu).

http://dx.doi.org/10.1016/j.apcatb.2014.12.023
0926-3373/

The semiconductor Bi_2WO_6 is utilized as a photocatalyst through inducing a series of reductive and oxidative reactions on its surface: when Bi_2WO_6 is irradiated by light possessing of photon energy ($h\nu$) greater than or equal to its band gap energy, the lone electron will be photo-excited and subsequently jumps to the conduction band. The photonic excitation leaves behind an empty unfilled valence band, and thus creating the electro-hole pair (e^-–h^+) and active species in subsequently. Despite three active species of ·OH, $O_2^{\bullet -}$ and h^+ can exist in Bi_2WO_6 photocatalysis simultaneously, there is a continuous controversy on the acting oxidative species regarding the morphology of Bi_2WO_6, the species of pollutants and the irradiation light source. For example, it was reported by Wang et al. [20] and Ding et al. [21] that the h^+ and O_2^- are the main active species in organic pollutants' degradation since Bi_2WO_6 can not generate ·OH in their reaction systems. However, Zhang et al. [22] discovered that ·OH radical is dominating active species in the disinfection of bacterial.

The mathematic model on intermediates' prediction, which ties together the experimental or field data into a more unified and understandable package, is very useful to predict chemical residual levels, undertake process control, design reactors, provide and compare management options, and train further engineers. Chu et al. [23] built a mathematic model to predict the intermeidates' accumulation in a photodechlorination process by consecutive irreversible reactions, which successfully puts forward a solution in decreasing side effect in a designed process. It was reported that, the intermediates in some processes are even harmful than the original pollutant [24]. For instance, our previous study found that the Bi_2WO_6 photocatalysis gave birth to harmful intermediates in the early stage of antibiotics degradation [25]. To solve this problem, the development of mathematic model can be used to avoid or abate the formation of unfavorable intermediates by simply controlling the experiment parameters.

In this study, we choose antibiotic norfloxacin as a model pollutant to systematically investigate the degradation mechanism of simulated solar light mediated Bi_2WO_6 process (SSL/Bi_2WO_6). The effect of a series of radical scavengers was studied to determine the actual active species and quantify their contributions. On the other hand, the aromatic intermediates were identified during the decay of norfloxacin by the proposed SSL/Bi_2WO_6 process. The reaction mechanism is clarified through examination of the probe decay in both direct SSL (sole simulated solar light irradiation) and SSL/Bi_2WO_6 process. Special attention has been paid to analyze the decay pathway that rule the process. Furthermore, a mathematical model was developed to predict the major intermediates' accumulation in the SSL/Bi_2WO_6 process, so that the intermediates level is predictable as the concentration of initial probe and reaction time is given.

2. Experiment

2.1. Chemical and reagents

All chemicals are of analytic reagent grade and used as received without further purification. Norfloxacin ($C_{16}H_{18}FN_3O_3$) purchased from Wako Pure Chemical Industries, Ltd. was used as the probe in this study. Bismuth tungstate was synthesized using tungsten acid (H_2WO_4), citric bismuth ($C_6H_5BiO_7$) and ammonia ($NH_3{\bullet}H_2O$) as precursors, which were purchased from Sigma–Aldrich Inc. The preparation method was illuminated in Supplementary Material and the characterization of Bi_2WO_6 was shown in Figure A1. The salts including potassium iodide (KI), sodium sulfate (Na_2SO_4), sodium nitrate ($NaNO_3$), sodium bicarbonate ($NaHCO_3$), ferric chloride ($FeCl_3$), and ferrous chloride ($FeCl_2$) were obtained from Sigma–Aldrich Inc. The mobile phase solvent for HPLC analysis (i.e., acetonitrile) came from Tedia Company. The pH level of mobile phase was adjusted by ammonium acetate (CH_3COONH_4), acetic acid (CH_3COOH) and/or orthophosphoric acid (H_3PO_4). A resistivity of 18.2 MΩ of distilled-deionized water was used for preparing mobile phase and stock solution, generated by a Bamstead NANOpure water treatment system (Thermo Fisher Scientific Inc. USA).

2.2. Experimental procedures

The degradation of norfloxacin was conducted in a simulated solar light photochemical reactor (Beijing Changtuo Company with a Xenon lamp of 300 W). The experiment setup and irradiation spectrum of Xenon lamp was shown in Figure A2 and A3 in Supplementary Material, respectively. Prior to the reaction, a predetermined amount of Bi_2WO_6 was added into 100 mL of norfloxacin solution in a quartz beaker/cylinder, and stirred in the darkness for 30 min to achieve adsorption equilibrium. After the equilibrium, the degradation was started by turning on the preheated light source. At preset intervals, exact 1 mL of sample was withdrawn and filtered through a 0.2 μm PTFE membrane for further analysis. All experiments were carried out in duplicate at room temperature (air-conditioned) at 23 ± 1 °C.

2.3. Analytical methods

The remaining norfloxain in solution was quantified by a high-performance liquid chromatography (HPLC), comprised with a Waters 515 pump, a Waters 2489 Dual λ absorbance detector and a Waters 717 plus autosampler. The norfloxacin in the solution was separated from its intermediates by a Restek C18 column (5.0 μm, 4.6 × 250 mm), and quantified at an adsorption wavelength of 280 nm. A mixture of 50% acetonitrile and 50% 0.025 mM orthophosphoric acid solution was chosen as the mobile phase running at a flow rate of 0.8 mL/min. Exact 10 μL of sample was injected for analysis.

The identification of aromatic intermediates was carried out at a Thermo Quest Finnigen LCQ Duo Mass spectrometer system, which was equipped with Thermo P4000 pumps, Thermo AS3000 autosampler with a 20 μL injection loop, UV6000LP photodiode array UV detector and an electrospray ionization with a quadruple ion-trap mass spectrometer operating at a positive mode (LC-ESI/MS). For the intermediates separation, a Varian Pursuit XRs C18 column (3.0 μm, 2.0 × 150 mm) was used. The mobile phase was comprised with two solutions: (A) 5 mM CH_3COONH_4 aqueous solution, adding CH_3COOH to adjust the pH to 4.6, and (B) acetonitrile. The composition of the mobile phase was changed according to the following gradient: 100% of A was kept during the first 2 min; from 2 to 50 min, B was linearly increased from 0 to 50%; from 50 to 60 min, B was continuous linearly increased to 100%. The flow rate of mobile phase was kept at 0.4 mL/min.

3. Results and discussion

3.1. Determining the active species in the SSL/Bi_2WO_6 process

The degradation of norfloxacin in SSL/Bi_2WO_6 process was illustrated in Fig. 1a. It was noted that 83.7% of norfloxacin was decomposed in 20 min. To clarify the role of active species in this process, KI and methanol was dosed into the reaction system for quenching the norfloxacin decay resulting from h^+ and ·OH oxidation, respectively [26,27]. Both scavengers showed negative effect on the norfloxacin decay: In the presence of KI, photogenerated h^+ are likely depleted by I^- capture via Eq. (1).

$$2h^+ + 2I^- \rightarrow I_2 \quad (1)$$

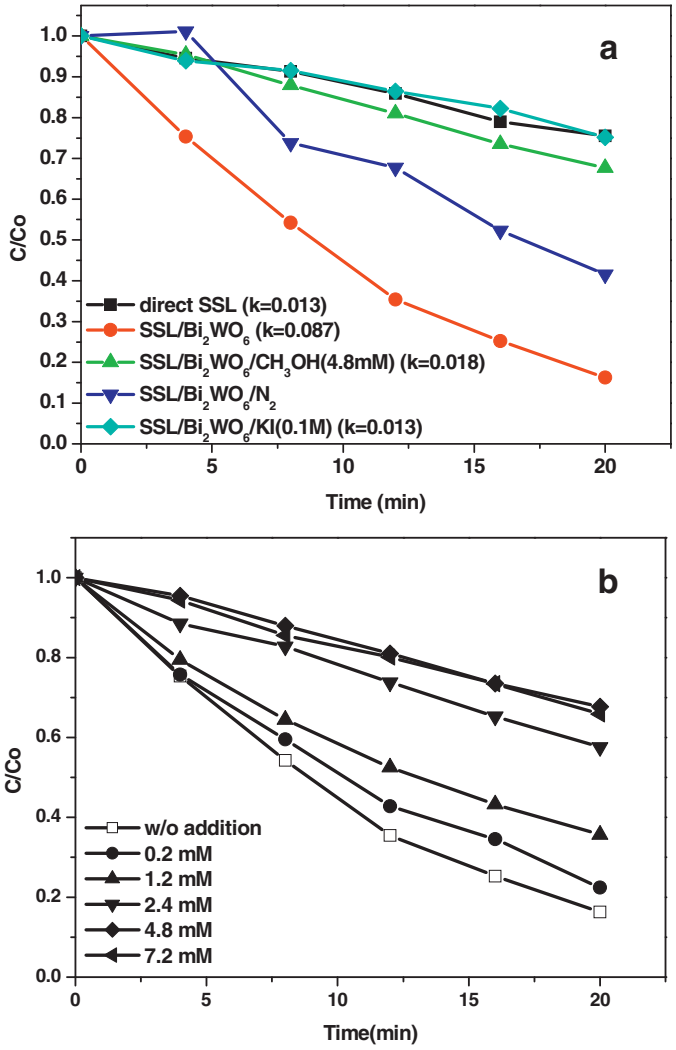

Fig. 1. Effect of (a) OH radical, hole and electron scavengers [all decay curves follow pseudo-first-order kinetics except SSL/Bi_2WO_6/N_2, k (rate constant, min^{-1})]; and (b) methanol at different concentrations.
Experiment conditions: $[Norfloxacin]_0$ = 0.0313 mM, $[Bi_2WO_6]$ = 0.5 g/L

It was noted that the norfloxacin decay curve in the presence of KI was almost the same to that of direct SSL, which indicated that the Bi_2WO_6 photocatalysis became talentless as h^+ was absent. This observation also suggested that the $O_2^{\bullet-}$ radical originated from e^- scavenging is a useless oxidant in our process. Its role is mainly an electron carrier to reduce the electron-hole recombination; The negative effect in the presence of methanol is resulted from methanol selectively quenching of ·OH radicals [28], which leads to the decrease of active species for norfloxacin decomposition. This result confirmed that ·OH radical is one of the active species in the SSL/Bi_2WO_6 process.Fig. 1b showed the norfloxacin decay performance at various [CH_3OH], where higher the [CH_3OH] greater the reduction of the degradation rate. It was interesting to find that the decay performance was level off when [CH_3OH] exceeded 4.8 mM, which indicated the ·OH radicals had been completely exhausted by overdosing methanol. Compared to the 83.7% of norfloxacin removal efficiency in control process (without dosing scavenger), when ·OH radicals were completely exhausted by methanol, the norfloxacin removal efficiency was decreased to 32.4% in 20 min. Undoubtedly, this retardation was entirely contributed to the ·OH oxidation. On the other hand, the difference between the process of SSL/Bi_2WO_6/KI and SSL/Bi_2WO_6/CH_3OH in Fig. 1a, should be resulted from the h^+ directly participating norfloxacin

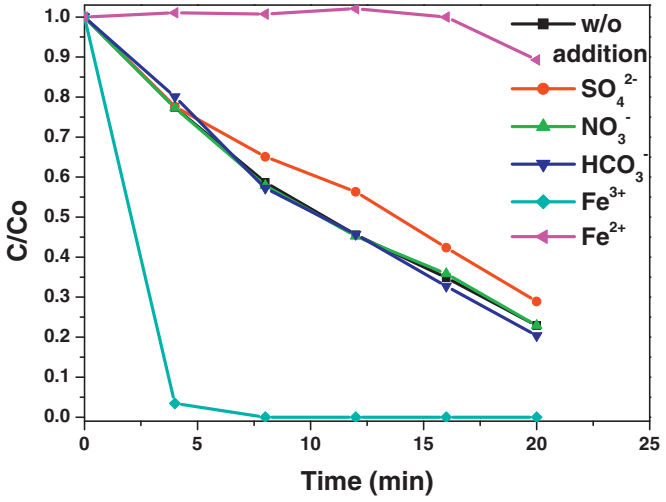

Fig. 2. Effect of anions and cations.
Experiment conditions: $[Norfloxcin]_0$ = 0.0313 mM, $[Bi_2WO_6]$ = 0.5 g/L. The concentrations of anions and canions are all of 10 mM

decomposition. As a result, the overall norfloxacin decay therefore is characterized into photolysis, photocatalysis-via hydroxyl radical, and photocatalysis-via direct hole oxidation, and their contribution is calculated to be 15.0, 79.3, and 5.7%, respectively (estimated from the contributions of pseudo-first-order decay rates). This finding demonstrated that the ·OH radicals played a major role in the SSL/Bi_2WO_6 process for norfloxacin decay.

Under the oxygen-free condition (SSL/Bi_2WO_6/N_2 process by purging N_2 gas), photogenerated e^- can not transferred efficiently, leading to a higher electron-hole recombination and a lower transformation efficiency of active species.

3.2. Effect of inorganic salts

Many studies have reported that the inorganic salts existing in water results in significant influence on the performance of pollutants treatment [29,30]. In this study, the effect of inorganic salts, including selected anions and cations were investigated. Fig. 2 showed the decay performance of norfloxacin in the presence of anions (NO_3^-, HCO_3^-, and SO_4^{2-}), and the results showed that a mild retardation occurred in the presence of SO_4^{2-}, while the anions of NO_3^- and HCO_3^- were inert to the SSL/Bi_2WO_6 process. The sulfate ion was reported to react with ·OH radical via Eq. (2) [31]:

$$SO_4^{2-} + {}^{\bullet}OH + H^+ \rightarrow {}^{\bullet}SO_4^- + H_2O \quad (2)$$

In this reaction, another weaker oxidizing agent sulfate radical ($^{\bullet}SO_4^-$) is formed associated with the consumption of ·OH radical. The sulfate radical is a selective radical and it has a larger molecular structure (than ·OH), which might hinder its chance to react with the probe. In addition, the formation of sulfate radical and subsequent reaction with the probe is a two-step process, which in theory will kinetically require longer time to react with the probe than that of ·OH radical. The mechanism results in a mild retardation of norfloxacin decay in the presence of SO_4^{2-}.

The NO_3^- apparently is inert in the process, but the HCO_3^- ion was reported as a ·OH radical scavenger (Eq. (3)) and frequently restrain photocatalytic reaction in previous literatures [32].

$$HCO_3^- + {}^{\bullet}OH \rightarrow CO_3^{\bullet-} + H_2O \quad (3)$$

However, an imperceptible influence in norfloxacin decay was observed in the presence of HCO_3^-. It was found that the pH level of reaction solution increased from neutral (6.7) to weak alkaline

Table 1
The information of the intermediates.

Product ID	Molecular ion, [M+ H+]	Proposed structure	Product ID	Molecular ion, [M+ H+]	Proposed structure
NO1*	322	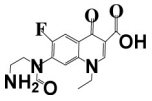	NO8	292	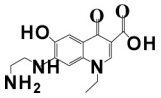
NO2*	322	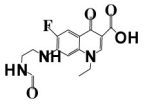	NO9*	279	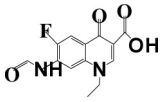
NO3	318	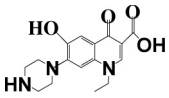	NO10	276	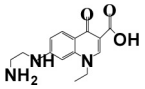
NO4*	334	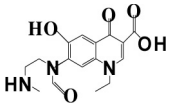	NO11	251	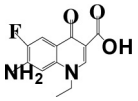
NO5	304	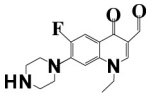	NO12*	261	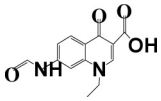
NO6	276	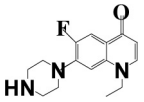	NO13	233	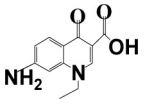
NO7	294	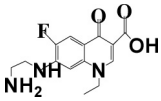	NO14	236	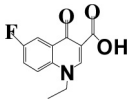

(9.2) after dosing 10 mM $NaHCO_3$ salt. In our previous study [25], the weak basic pH condition is favored by the SSL/Bi_2WO_6 process, because the higher [OH^-] improves the formation of ·OH radicals via Eq. (2). As a result, the imperceptible change between the presence and absence of HCO_3^- is likely ascribed to the joint result of scavenger retardation and pH level amelioration. In addition, the norfloxacin decay performance in the presence of SO_4^{2-} and HCO_3^- reconfirms the importance of ·OH radical in the SSL/Bi_2WO_6 process.

The performances of norfloxacin decay in the presence of cations Fe^{3+} and Fe^{2+} were also evaluated, and the result was shown in Fig. 2. It can be noted that a dramatic promotion with 95% of norfloxacin removal was achieved in 5 min in the presence of Fe^{3+}, while the process was almost totally terminated in the first 15 min in the presence of Fe^{2+}. It was known that Fe^{3+} is an efficient electron acceptor [15], which effectively separate photo-generated electron-hole pairs and increase the yield of photogenerated active species. Besides, it was noted that the solution pH level was decreased from neutral to acidic (pH 3.5) after Fe^{3+} salt was dosed. At acidic condition (pH 2.5–5.0), $Fe(OH)^{2+}$ is the dominant photoreactive species in ferric solution, which produces ·OH radical via its photolysis according to the following reaction in Eq. (4) [33];

$$Fe(OH)^{2+} \xrightarrow{h\nu} Fe^{2+} + {}^{\bullet}OH \quad (4)$$

This generated ·OH radical also involves in the norfloxacin decomposition, which results in the improvement of SSL/Bi_2WO_6 process via increasing the concentration of active species.

For the ferrous ions, the retardation in the first 15 min suggests that the Bi_2WO_6 photocatalysis is completely inhibited by the Fe^{2+} ions. This is because the Fe^{2+} is an effective hole scavenger (Eq. (5)),

$$Fe^{2+} + h^+ \rightarrow Fe^{3+} \quad (5)$$

After 15 min, however the norfloxacin started to decompose slowly, it is a good evidence to justify both the proposed Fe^{3+} and Fe^{2+} mechanisms, where the accumulation of enough [Fe^{3+}] in the solution is capable of initiating the accelerated norfloxacin decay as previously discussed.

3.3. Transformation mechanism of norfloxacin by SSL/Bi_2WO_6 process

The transformation and/or degradation mechanism of norfloxacin in the proposed SSL/Bi_2WO_6 process was investigated. The intermediates were identified on the basis of molecular ions and mass fragment ions detected by MS spectrum. Fourteen (14) intermediates were identified in the SSL/Bi_2WO_6 process. The information of the intermediates including the protonated ion ([M+ H^+]) and proposed molecular structure was summarized in Table 1. From the structure of intermediates, it was found that the products NO1, NO2, NO7, and NO11 with *m/z* of 322, 322, 294, and 251, respectively, arise from partial elimination of the piperazine ring. The intermediate NO3 with *m/z* 318 was attributed to the F atom replacement by hydroxyl ion. The cleaved fragment with *m/z* [M + H-16]$^+$ and *m/z* [M + H-44]$^+$, corresponding to the loss of hydroxyl ion and CO_2, result in the generation of intermediates NO5 and NO6, respectively.

The evaluation profile of the fourteen intermediates was organized in peak area and shown in Fig. 3. The intermediates NO1 and NO2 were integrated because they are isomers produced from the same reaction. As illuminated in Fig. 3, compound NO1 and NO2 apparently were the primary intermediates, which showed dramatic increment and drop within the first 2 h. NO7 was likely the secondary intermediate because its peak concentration showed up immediately after the primary intermediates. Other major intermediates, such as NO9, NO10, NO11, and NO13, should be the

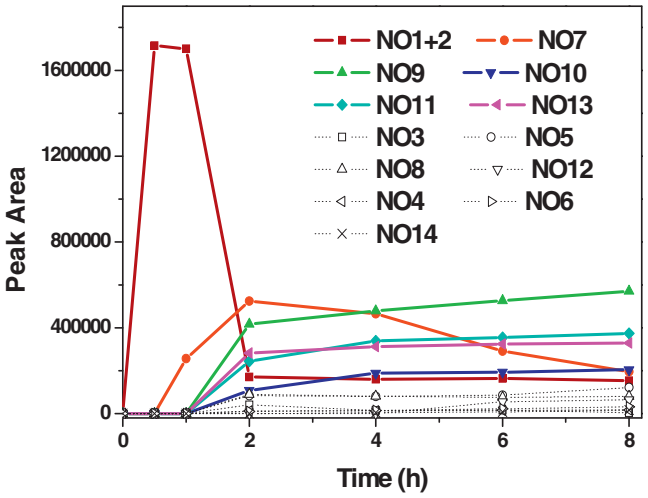

Fig. 3. The evaluate profile of SSL/Bi_2WO_6 process.
Experiment conditions: $[Norfloxcin]_0$ = 0. 3130 mM, $[Bi_2WO_6]$ = 2 g/L

intermediates of final/late stage because they all possessed continuous accumulations during the test. The decay pathway was thereby derived as shown in Fig. 4. The degradation of norfloxacin was mainly initiated by piperazine ring transformation (Pathway 1, P1), defluorination (Pathway 2, P2), and decarboxylation (Pathway 3, P3). In Pathway 1, NO1 and NO2 are both obtained from the hydroxyl oxidation at the 2′ and 3′-carbon of piperazine, following by the structure rearrangement and the generation of amide (with —NH—CH=O group). In particular, the formation of NO1 and/or NO2 cannot be achieved in one step. It should be derived from the sequential attack of ·OH radicals at the 2′ and 3′ carbon in piperazine ring, which gave birth to compound with *m*/*z* of 336 and then 350, respectively. Then after, the ·OH reaction induced the decarbonylation in the amide (of compound with *m*/*z* of 350). As a result, NO1 and/or NO2 were produced showing a functional group of amine (R—NH_2). Similar reaction pathway has been reported in the reaction between piperazine ring and ·OH radicals in TiO_2 photocatalysis [34], and the intermediates equivalent to the role of compounds with *m*/*z* of 336 and 350 were detected in TiO_2 photocatalysis. The absence of compounds 336 and 350 in the SSL/Bi_2WO_6 process might be due to their shorter lifetime when the ·OH radical is abundance at the beginning of the degradation. The further ·OH oxidation led to the further decarbonylation and the generation of NO7. From NO7 to NO11, the amine with functional group of —NH—CH_2—CH_2—NH_2 (NO7) was oxidized to amide —NH—CH=O (NO9) and then decarbonylated to amine —NH_2 (NO11). Obviously, this piperazine oxidation in SSL/Bi_2WO_6 process can thereby be described by the following sequence reactions (Eq. (6)).

$$\ldots - NH - C - \ldots \xrightarrow{+^{\bullet}OH} \ldots - NH - CH = O \xrightarrow{+^{\bullet}OH} [\ldots - NH - \dot{C} = O \xrightarrow{+^{\bullet}OH} \ldots] - N H_2 \quad (6)$$

In particular, NO9 was reported as the first time in this study, which provide a solid evidence of the involvement of ·OH radicals in the SSL/Bi_2WO_6 process because the formation of carbonyl group is one of the characteristics of ·OH reaction [34]. Besides, piperazine oxidation via above routes in Eq. (6) was also observed in the degradation Pathway 2, from NO3 to NO4 and NO8, and from NO10 to NO12.As a comparison, the norfloxaxin degradation in the absence of Bi_2WO_6 (direct SSL) was also investigated. Nine (9) of intermediates in Table 1 were detected, while the five amide intermediates (with the functional group of —NH—CH=O) that found in SSL/Bi_2WO_6 process were not detected (as marked * in both Fig. 4 and Table 1). The norfloxacin degradation in the direct SSL process also involved piperazine ring transformation, defluorination, and decarboxylation. The intermediates profile and decay pathway was shown in Figure A4 and Figure A5 (Supplementary material), respectively. Similar to the SSL/Bi_2WO_6 process, the norfloxacin degradation can be divided into three sub-pathways as well. However, there is a major difference in piperazine transformation owing to the absence of the amide intermediates. As a result, the piperazine transformation in the direct SSL process followed another decay pathway as below,

$$\ldots - N H - C - \ldots \xrightarrow{+SSL} \ldots - NH_2 \quad (7)$$

The mechanism difference between SSL/Bi_2WO_6 and SSL is apparently ascribed to the involvement of Bi_2WO_6 photocatalysis. Considering the ·OH radical is the main active species in the SSL/Bi_2WO_6 process, the disappearance of transition amide compounds with functional group of —NH—CH=O is due to the lack of ·OH radical in the SSL process.

In SSL/Bi_2WO_6 process, it can be calculated from the peak area that about 53.3, 18.1, and 0.9% of total norfloxacin was removed via piperazine ring transformation (Sum of products' peak area from piperazine ring transformation/Peak area of initial norfloxacin), defluorination (Sum of products' peak area from defluorination/Peak area of initial norfloxacin), and decarboxylation (Sum of products' peak area from decarboxylation/Peak area of initial norfloxacin), respectively at 2 h. Meanwhile, a corresponding contribution via the direct SSL process was 34.9, 17.9 and 0.8%, respectively. It can be inferred that, Bi_2WO_6 photocatalysis obviously promote the piperazine ring transformation. This observation demonstrated that the dominate reaction site attracted by ·OH radicals is the piperazine of norfloxacin.

On the other hand, the Bi_2WO_6 photocatalysis showed imperceptible effects on the defluorination and decarboxylation, because these two processes are totally ascribed the direct SSL photolysis. The defluorination occurred via hydroxyl substitution (from norfloxacin to NO3) should come from the fluorine hydrolysis, whereas via direct reduction (from NO7 to NO10) should be ascribed to photodehalogenation [35,36]. The emergence of NO5 and NO6 showed the loss of hydroxyl and CO_2 in the carboxyl group. NO5 and NO6 exhibited a similar accumulation levels in both the direct SSL and SSL/Bi_2WO_6 processes, suggesting the Pathway 3 was dominated by direct photodecomposition.

3.4. Development of mathematic model

Due to the lack of authentic standards in the market, currently the concentration of intermediates cannot be reported better than using their peak areas/highs. From the TOC test result, 0.0, 0.4, 7.0, 11.9, and 15.5% of TOC was reduced in 1, 2, 4, 6, and 8 h, respectively. It can be deduced that these minor TOC deductions should be totally ascribed to the carbon loss on the side chains, and no benzene-ring opening in the SSL/Bi_2WO_6 process within 8 h. Therefore, an arithmetic scheme by combining benzene-ring balance and the Beer-Lambert law (Eq. (8)) was proposed to solve the concentration of major intermediates assuming (a) there is no benzene-ring loss in the process (confirmed by the TOC analysis), (b) the concentration of intermediates are linear to their peak areas/highs, and (c) the mass contributed by minor intermediates are negligible, so that the molar absorptivity and/or concentration of the major intermediates become calculable.

$$A = \xi C L \quad (8)$$

where *A* is absorbance, ξ represents the molar absorptivity ($L \cdot mol^{-1} \cdot cm^{-1}$), *C* is the concentration of compound ($mol \cdot L^{-1}$), and L is the path length (cm). Because L is fixed in HPLC analysis, the

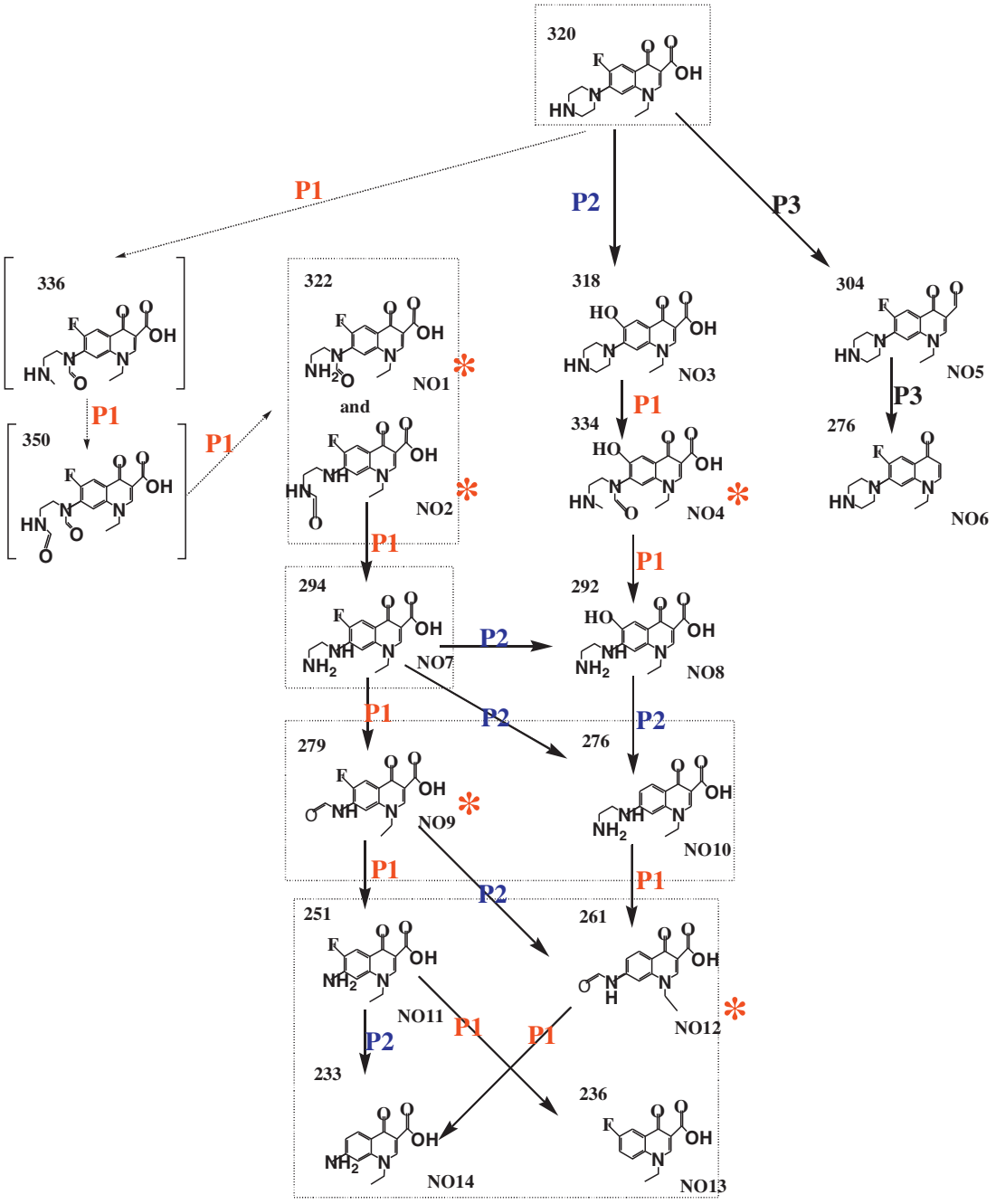

Fig. 4. Degradation pathway of Bi_2WO_6/SSL process
(Compounds labeled with asterisk comes from hydroxyl radicals' reaction; P1 – Pathway 1 form piperazine ring transformation, P2 – Pathway 2 from defluroination, and P3 – Pathway 3 from decarboxylation)

absorbance of intermediates at any time point (t_x) can be integrated into the following equation (Eq. (9)) based on the principle of mass balance:

$$A_{\mathrm{Nor}(t=0)} = A_{\mathrm{Nor}(t_x)} + \frac{A_{\mathrm{int_1}(t_x)}}{\xi_{\mathrm{int_1}}/\xi_{\mathrm{nor}}} + \frac{A_{\mathrm{int_{2(t_x)}}}}{\xi_{\mathrm{int_2}}/\xi_{\mathrm{Nor}}} \ldots + \frac{A_{\mathrm{int_n}}(t_x)}{\xi_{\mathrm{int_n}}/\xi_{\mathrm{Nor}}} \quad (9)$$

where A_{Nor} and A_{int} is the absorbance (i.e., peak area) of norfloxacin and intermediates, respectively. The ξ_{Nor} and ξ_{int} represents the molar absorptivity of norfloxaicn and intermediates, respectively.

After putting the experiment data (A_{Nor} and A_{int} at 0.5, 1, 2, 4, 6, and 8 h) into above Eq. (9), six formulas were built up where $\xi_{\mathrm{int}}/\xi_{\mathrm{Nor}}$ is unknown. Since the degradations via defluorination and decarboxylation are minor, the items/absorbance concern about NO3, 4, 5, 6, 8, 12, and 14 were neglected. As a result, the remaining six unknown $\xi_{\mathrm{int}}/\xi_{\mathrm{Nor}}$ from NO1 + 2 (isomers), NO7, NO9, NO10, NO11, and NO13 are calculable and show the value of 3.0, 0.18, 0.38, 0.42, 0.50, and 0.51, respectively. Based on the determined ξ_{Nor} of 1.39×10^{10} peak area·L·mol^{-1}·cm^{-1} in this study [37], the concentration of each major intermediate was calculable and the result was shown in Fig. 5 (as the data points).

Meanwhile, after ignoring the minor intermediates and rearranging the major intermediates into groups (see the dotted line box in Fig. 4), the norfloxacin decay became predicable by using

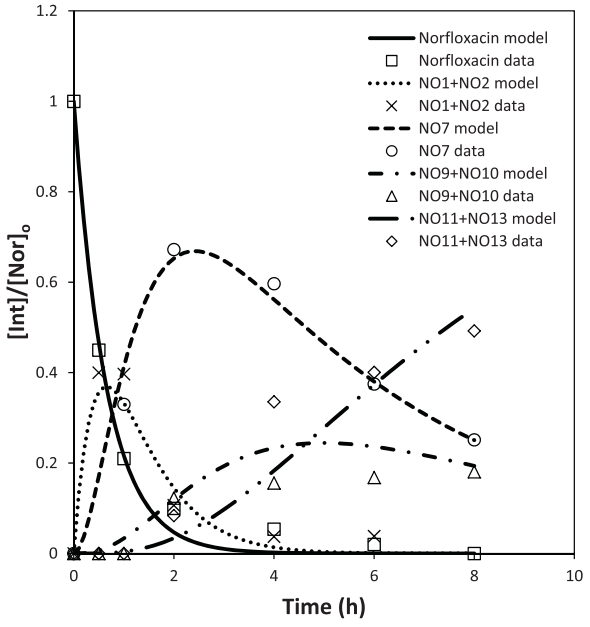

Fig. 5. Comparison between the experimental (calculated) data and the predicted result from the proposed models.

a consecutive irreversible reactions as proposed in the following Scheme,

$$\text{Norfloxacin} \xrightarrow{k_1} \text{NO1, NO2} \xrightarrow{k_2} \text{NO7} \xrightarrow{k_3} \text{NO9, NO10} \xrightarrow{k_4} \text{NO11, NO13}$$

Assuming each of the above step follows pseudo first-order kinetics with the rate constants noted by k_1–k_4. The concentration of intermediates in each step is formulated by first order differential equations as shown in Eqs. (10)–(13) [23].

$$A_{\text{Nor}(t=0)} = A_{\text{Nor}(t_x)} + \frac{A_{\text{int}_1(t_x)}}{\xi_{\text{int}_1}/\xi_{\text{nor}}} + \frac{A_{\text{int}_{2(t_x)}}}{\xi_{\text{int}_2}/\xi_{\text{Nor}}} \ldots + \frac{A_{\text{int}_n}(t_x)}{\xi_{\text{int}_n}/\xi_{\text{Nor}}} \quad (10)$$

$$[\text{NO1, NO2}] = \frac{k_1[\text{N orfloxacin}]_0}{k_2 - k_1}[e^{-k_1 t} - e^{-k_2 t}] \quad (11)$$

$$[\text{NO7}] = [\frac{k_1 k_2[\text{Norfloxacin}]_0 e^{-k_1 t}}{(k_2 - k_1)(k_3 - k_1)}] + [\frac{k_1 k_2[\text{Norfloxacin}]_0 e^{-k_2 t}}{(k_1 - k_2)(k_3 - k_2)}] + [\frac{k_1 k_2[\text{Norfloxacin}]_0 e^{-k_3 t}}{(k_1 - k_3)(k_2 - k_3)}] \quad (12)$$

$$[\text{NO9, NO10}] = [\frac{k_1 k_2 k_3[\text{Norfloxacin}]_0 e^{-k_1 t}}{(k_2 - k_1)(k_3 - k_1)(k_4 - k_1)}] + [\frac{k_1 k_2 k_3[\text{Norfloxacin}]_0 e^{-k_2 t}}{(k_1 - k_2)(k_3 - k_2)(k_4 - k_2)}] + [\frac{k_1 k_2 k_3([\text{Norfloxacin}])_0 e^{-k_3 t}}{(k_1 - k_3)(k_2 - k_3)(k_4 - k_3)}] + [\frac{k_1 k_2 k_3[\text{Norfloxacin}]_0 e^{-k_4 t}}{(k_1 - k_4)(k_2 - k_4)(k_3 - k_4)}] \quad (13)$$

The model curves can be fit to the experimental (calculated) data quite well by trial and error, as shown in Fig. 5. The rate constant of each step k_1, k_2, k_3, and k_4 can be resolved as 1.525, 1.519, 0.207, and 0.401 h^{-1}, respectively. The intermediates accumulation is now predictable as the concentration of initial norfloxacin and reaction time is selected, which is very useful in practical wastewater treatment.

The toxicity examination in our process shows that the harmful intermediates appeared in 2 h and arrived to an ineffective level in 6 h (See Appendix Figure A6). By fitting this result with the accumulation curve in Fig. 5, it can be determined that the harmful intermediates are compounds NO1 and NO2. Our developed mathematic model points out that the unexpected NO1 and NO2 reached the highest level in 0.6 h and completely decomposed in 6 h in the SSL/Bi_2WO_6 process. This observation provides helpful suggestions to decrease the side effect of toxicity by simply control the experiment parameters (i.e., reaction time).

4. Conclusions

The ·OH radical plays a major role in the decomposition of norfloxacin in the SSL/Bi_2WO_6 process. The overall efficiency of photolysis, photocatalysis-via hydroxyl radical, and photocatalysis-via direct hole oxidation was 15.0, 79.3, and 5.7%, respectively. The $O_2^{\bullet -}$ radicals originated from photogenerated e^- is a useless oxidant, its role is mainly an electron carrier to reduce the electron-hole recombination. The role of ·OH and h^+ was further confirmed by the effect of inorganic ions of SO_4^-, HCO_3^-, Fe^{3+} and Fe^{2+}. There are three decay pathways for norfloxacin: piperazine ring transformation, defluorination, and decarboxylation. The comparison of norfloxacin decay by direct SSL with SSL/Bi_2WO_6 process demonstrated that the five amide intermediates were all derived from ·OH radicals, and the ·OH oxidation formula was described by the Eq. (6). A mathematical model was developed to predict the major intermediates' accumulation in the process, so that the concentration of intermediates is predictable as the concentration of initial probe and reaction time is given.

Acknowledgement

The authors are grateful for the financial support of the research grant from the Hong Kong Polytechnic University (PRHC and G-YN93) of Hong Kong, China.

Appendix A. Supplementary data

Supplementary data associated with this article can be found, in the online version, at http://dx.doi.org/10.1016/j.apcatb.2014.12.023.

References

[1] S. Simoens, J. Verhaegen, P. van Bleyenbergh, W.E. Peetermans, M. Decramer, Antimicrob. Agents Chemother. 55 (2011) 3051–3053.
[2] X.S. Chang, M.T. Meyer, X.Y. Liu, Q. Zhao, H. Chen, J.A. Chen, Z.Q. Qiu, L. Yang, J. Cao, W.Q. Shu, Environ. Pollut. 158 (2010) 1444–1450.
[3] A. Albini, S. Monti, Chem. Soc. Rev. 32 (2003) 238–250.
[4] G. Rigos, I. Nengas, M. Alexis, G.M. Troisi, Aquat. Toxicol. 69 (2004) 281–288.
[5] A. Gulkowska, H.W. Leung, M.K. So, S. Taniyasu, N. Yamashita, L.W.Y. Yeung, B.J. Richardson, A.P. Lei, J.P. Giesy, P.K.S. Lam, Water Res. 42 (2008) 395–403.
[6] T.P.H. Phan, S. Managaki, N. Nakada, H. Takada, A. Shimizu, D.H. Anh, P.H. Viet, S. Suzuki, Sci. Total Environ. 409 (2011) 2894–2901.
[7] Y.-J. Lee, S.-E. Lee, D.S. Lee, Y.-H. Kim, Environ. Toxicol. Pharmacol. 26 (2008) 216–221.
[8] K. Oberlé, M.-J. Capdeville, T. Berthe, H. Budzinski, F. Petit, Environ. Sci. Technol. 46 (2012) 1859–1868.
[9] A.L. Linsebigler, G. Lu, J.T. Yates, Chem. Rev. 95 (1995) 735–758.
[10] M. Chen, W. Chu, J. Hazard. Mater. 219–220 (2012) 183–189.
[11] Y. Zhang, P. Zhang, Y. Huo, D. Zhang, G. Li, H. Li, Appl. Catal. B: Environ. 115–116 (2012) 236–244.
[12] M. Pelaez, P. Falaras, V. Likodimos, A.G. Kontos, A.A. de la Cruz, K. O'Shea, D.D. Dionysiou, Appl. Catal. B: Environ. 99 (2010) 378–387.
[13] S. Yang, L. Lou, K. Wang, Y. Chen, Appl. Catal. A: Gen. 301 (2006) 152–157.
[14] X.-R. Xu, S.-X. Li, X.-Y. Li, J.-D. Gu, F. Chen, X.-Z. Li, H.-B. Li, J. Hazard. Mater. 164 (2009) 527–532.
[15] G.R. Bamwenda, T. Uesigi, Y. Abe, K. Sayama, H. Arakawa, Appl. Catal. A: Gen. 205 (2001) 117–128.
[16] Z. Ai, Y. Huang, S. Lee, L. Zhang, J. Alloys Compd. 509 (2011) 2044–2049.
[17] X. Wang, G. Li, H. Zhu, J.C. Yu, X. Xiao, Q. Li, Appl. Catal. B: Environ. 147 (2014) 17–21.
[18] G. Li, D. Zhang, J.C. Yu, M.K.H. Leung, Environ. Sci. Technol. 44 (2010) 4276–4281.
[19] M. Shang, W.Z. Wang, S.M. Sun, L. Zhou, L. Zhang, J. Phys. Chem. C 112 (2008) 10407–10411.

[20] C. Wang, H. Zhang, F. Li, L. Zhu, Environ. Sci. Technol. 44 (2010) 6843–6848.
[21] X. Ding, K. Zhao, L. Zhang, Environ. Sci. Technol. 48 (2014) 5823–5831.
[22] L.-S. Zhang, K.-H. Wong, H.-Y. Yip, C. Hu, J.C. Yu, C.-Y. Chan, P.-K. Wong, Environ. Sci. Technol. 44 (2010) 1392–1398.
[23] W. Chu, J.R. Hunt, C.T. Jafvert, Water Res. 36 (2002) 843–850.
[24] M. DellaGreca, A. Fiorentino, M.R. Iesce, M. Isidori, A. Nardelli, L. Previtera, F. Temussi, Environ. Toxicol. Chem. 22 (2003) 534–539.
[25] M. Chen, W. Chu, Ind. Eng. Chem. Res. 51 (2012) 4887–4893.
[26] R. Palominos, J. Freer, M.A. Mondaca, H.D. Mansilla, J. Photochem. Photobiol. A 193 (2008) 139–145.
[27] M. Cho, H. Chung, W. Choi, J. Yoon, Water Res. 38 (2004) 1069–1077.
[28] Y.-P. Chin, P.L. Miller, L. Zeng, K. Cawley, L.K. Weavers, Environ. Sci. Technol. 38 (2004) 5888–5894.
[29] M. Sökmen, A. Özkan, J. Photochem. Photobiol. A 147 (2002) 77–81.
[30] C. Guillard, H. Lachheb, A. Houas, M. Ksibi, E. Elaloui, J.-M. Herrmann, J. Photochem. Photobiol. A 158 (2003) 27–36.
[31] K.-H. Wang, Y.-H. Hsieh, C.-H. Wu, C.-Y. Chang, Chemosphere 40 (2000) 389–394.
[32] G.V. Buxton, A.J. Elliot, Int. J. Radiat. Appl. Instrum. C Radiat. Phys. Chem. 27 (1986) 241–243.
[33] H. Mestankova, G. Mailhot, J. Jirkovsky, J. Krysa, M. Bolte, Environ. Chem. Lett. 7 (2009) 127–132.
[34] T. An, H. Yang, W. Song, G. Li, H. Luo, W.J. Cooper, J. Phys. Chem. A 114 (2010) 2569–2575.
[35] Y.R. Wang, W. Chu, Appl. Catal. B: Environ. 123–124 (2012) 151–161.
[36] W. Chu, C.T. Jafvert, C.A. Diehl, K. Marley, R.A. Larson, Environ. Sci. Technol. 32 (1998) 1989–1993.
[37] A.H. Aktas, S. Goksu, Rev. Anal. Chem. 29 (2010) 81–91.